HHS Public Access

Author manuscript

J Alzheimers Dis. Author manuscript; available in PMC 2025 January 02.

Published in final edited form as:

J Alzheimers Dis. 2022 ; 88(1): 323–334. doi:10.3233/JAD-215477.

BDNF and *KIBRA* polymorphisms are related to altered resting state network connectivity in middle age

Jenna Katherine Blujus[a], **Laura Elizabeth Korthauer**[a,b,c], **Elizabeth Awe**[a,d], **Marijam Frahmand**[a], **Ira Driscoll**[a,*]

[a]Department of Psychology, University of Wisconsin-Milwaukee, Milwaukee, WI

[b]Department of Psychiatry and Human Behavior, Alpert Medical School of Brown University, Providence, RI[

[c]Department of Psychiatry, Rhode Island Hospital, Providence, RI

[d]Department of Neurology, Medical College of Wisconsin, Milwaukee, WI

Abstract

Background: Disease-modifying treatments for Alzheimer's disease (AD) may be more successful if interventions occur early, prior to significant neurodegeneration and subsequent to the onset of clinical symptoms, potentially during middle age. Polymorphisms within *BDNF*, *COMT*, and *KIBRA* have been implicated in AD and relate to episodic memory and executive functioning, two domains that decline early in AD.

Objective: The purpose of the current study was to use an endophenotype approach to examine in healthy, non-demented middle-aged adults the association between polymorphisms in *BDNF*, *COMT*, and *KIBRA* and functional connectivity within networks related to episodic memory and executive function (i.e., default mode network (DMN), executive control network (ECN), and frontoparietal network (FPN)).

Methods: Resting state networks were identified using independent component analysis and spatial maps with associated time courses were extracted using a dual regression approach.

Results: Functional connectivity within the DMN was associated with polymorphisms in *BDNF* (rs11030096, rs1491850) and *KIBRA* (rs1030182, rs6555791, rs6555802) (p's < .05), ECN connectivity was associated with polymorphisms in *KIBRA* (rs10475878, rs6555791) (p's < .05), and FPN connectivity was associated with *KIBRA* rs6555791 (p < .05). There were no *COMT*-related differences in functional connectivity of any of the three networks investigated (p's > .05).

Conclusion: Our study demonstrates that in middle age, polymorphisms in *BDNF* and *KIBRA* are associated with altered functional connectivity in networks that are affected early in AD.

*Correspondence: Dr. Ira Driscoll; Department of Psychology, University of Wisconsin-Milwaukee; 2441 E Hartford Ave, Milwaukee, WI 53211; driscoli@uwm.edu.

CONFLICT OF INTEREST/DISCLOSURE STATEMENT

The authors have no conflict of interest to report.

Future preclinical work should consider these polymorphisms to further elucidate their role in pathological aging and to aid in the identification of biomarkers.

Keywords

Middle Aged; Functional Neuroimaging; Endophenotypes; Alzheimer Disease; Genetic Polymorphism; Brain-Derived Neurotrophic Factor

INTRODUCTION

Dementia is characterized by impairment in multiple cognitive domains including learning and memory, language, and executive functioning, which significantly impacts independence [1]. Alzheimer's disease (AD), the most common form of dementia, is associated with two neuropathological hallmarks, amyloid-ß (Aß) plaques and neurofibrillary tangles, along with progressive cognitive decline, particularly in learning and memory [1]. The treatments that are currently available are largely ineffective because by the time of diagnosis, when treatments are typically delivered, pathology and neurodegeneration are significant and may be irreversible [2]. As the prevalence of AD is projected to more than double by 2050 [3], identifying preclinical biomarkers that can pinpoint individuals most susceptible to AD will be essential to improve early intervention and treatment outcomes.

Episodic memory and executive function, two complex polygenic cognitive domains [4, 5], are affected early in the course of AD, with accelerated decline in each cognitive domain evident three to seven years prior to diagnosis [6, 7]. Single nucleotide polymorphisms (SNP) in genes that contribute to such cognitive functions, including *BDNF*, *COMT*, and *KIBRA*, have also been implicated in AD [8–13] by altering the functioning or availability of gene products, ultimately affecting cognitive function in domains vulnerable to AD. *KIBRA* and *BDNF* are both highly expressed in the hippocampus [14, 15], an area that supports learning and memory. Polymorphisms in *KIBRA* and *BDNF* are related to the variability observed in episodic memory performance [15, 16]. *COMT*, which encodes an enzyme that breaks down dopamine in the prefrontal cortex, is related to executive function [13]. While the measurable impact of polymorphisms within *BDNF*, *COMT*, and *KIBRA* on cognition is expected to be minimal, investigating intermediate phenotypes, such as functional brain integrity, may reveal more direct associations between genes and behavior and uncover unique neural pathways that underlie cognitive dysfunction.

Mounting evidence suggests the promise of resting state fMRI as a biomarker of AD during preclinical and clinical stages [17–19]. Examining functional connectivity of distinct brain networks which underlie memory and executive function, such as the default mode network (DMN), executive control network (ECN), and frontoparietal network (FPN), could be a particularly useful intermediate phenotype. The DMN contains a few major cortical hubs, including the precuneus, posterior cingulate cortex (PCC), and prefrontal cortex, and is the most-well characterized network in aging and AD [20]. The DMN can be parcellated into two subnetworks consisting of anterior (aDMN) and posterior (pDMN) divisions [21–23]. Each subnetwork is differentially related to cognition; the aDMN supports self-referential thought while the pDMN is related to episodic memory [21]. Compared to healthy controls,

AD patients exhibit higher aDMN but lower pDMN connectivity [22, 24–26]. The PCC and precuneus, two hub regions in the pDMN, are especially vulnerable to AD pathology [27], and connectivity of these regions is among the first to be disrupted in AD [26], though the direction of findings in preclinical stages (i.e., hyperconnectivity vs. hypoconnectivity) is inconsistent [23, 26, 28]. In addition to the DMN, both the FPN and ECN are related to executive function and working memory [29], and functional connectivity within these networks is disrupted in disease [24, 30, 31]. Compared to healthy controls and mild cognitive impairment patients, individuals with AD show higher connectivity within the ECN [24, 31], while connectivity of the FPN is altered in both directions, as frontal regions exhibit hypoconnectivity while parietal regions exhibit hyperconnectivity [24].

Most existing studies employing a genetic imaging approach examined the relationship between *APOE* ε4 (*APOE4*), the greatest genetic risk factor for AD, and functional brain integrity [32–36], though findings in middle age are equivocal. Our group recently demonstrated that in a healthy middle-aged sample, *APOE4*-related differences were only evident when using more sensitive techniques such as examining graph properties on a combined functional-structural network [35] rather than conventional resting state network metrics [36]. Moving beyond *APOE4*, few studies have examined the relationship between polymorphisms in genes associated with cognitive function (*BDNF*, *COMT*, *KIBRA*) and network connectivity [37–40], especially in the context of aging and AD. Moreover, middle age, a time period when AD pathophysiology has likely begun but clinical symptoms are not yet expressed, has largely been omitted from investigations to date. In the current study, the purpose was to expand our previous work and examine genes outside of *APOE* associated with cognitive function in domains vulnerable to AD, including *BDNF*, *COMT*, and *KIBRA*, and their relationship with functional connectivity within the DMN, ECN, and FPN in healthy, non-demented middle-aged adults (see Table 1). We predicted that healthy, non-demented middle-aged carriers of alleles in *BDNF*, *COMT*, and *KIBRA* that have been linked to worse cognitive performance and implicated in AD would show altered connectivity within the DMN, ECN, and FPN, with risk carriers exhibiting more AD-like connectivity patterns compared to non-risk carriers. Identifying genotype-related alterations in connectivity in middle age is critical for improving the characterization of biomarkers with potential for preclinical detection of AD.

MATERIALS AND METHOD

Participants

Participants were 123 adults from the Milwaukee community (age 40 – 60; M = 50.03, SD = 6.03, 49 males). Participants were in general good health and did not have any history of neurological conditions (e.g., stroke, dementia, Parkinson's disease, epilepsy), psychiatric disorders (e.g., schizophrenia, bipolar disorder), severe cardiac disease (e.g., angioplasty, coronary bypass surgery), metastatic cancer, or substance use disorder. All participants met the following inclusion criteria: cognitively normal based on Mattis Dementia Rating Scale Second Edition [41] ≥ 136; Mini Mental State Exam [42] ≥ 25; and non-depressed (Geriatric Depression Scale [43] ≤ 10. All adults gave informed consent and were compensated financially for their participation. The study was approved by and conducted in accordance

with the guidelines of the University of Wisconsin-Milwaukee and the Medical College of Wisconsin institutional review boards.

Genotyping

The three genes were selected for analysis based on their promising associations with cognitive domains vulnerable to pathological aging and risk for AD [8–13, 15, 16]. Haplotype tagging SNPs (tSNPs) were selected from the International Haplotype Map project (www.hapmap.org) using a bulk download of tag SNP data. To ensure robust haplotype tagging within the cohort, SNPs were selected based upon a pairwise r^2 of greater than 0.8 and a minor allele frequency of greater than 0.2, all based on CEPH Caucasian data typed as a part of the HapMap project. The regions of the genome containing all exons of *BDNF*, *KIBRA*, and *COMT* plus at least 20kb of 5' and 3' flanking sequence were selected for tSNP analysis. This produced a list of 28 SNPs required to tag the genes of interest. In addition to these SNPs, we also assayed polymorphisms that make up the common ε2, ε3 and ε4 APOE genotypes (rs7412 and rs429358) and other well-established non-synonymous alterations in COMT (rs4680) and BDNF (rs6265) to produce a total of 32 SNPs to be assayed (Table 7).

All assays were performed at the University of Wisconsin Biotechnology Core Facility, using a custom Illumina GoldenGate assay. DNA was obtained from a blood sample (10mL) from each participant. Each GoldenGate assay required 250ng of genomic DNA and each assay was run in a 96-well plate format. Each plate consisted of 92 study samples and four replicate samples from CEPH families 1347 and 1331 to provide quality assurance of plate orientation and genotype reproducibility. Genotype calling was performed using the algorithms within BeadStudio (Illumina Inc, San Diego CA), and genotype cluster files were generated using a minimum of 1,000 individuals. See Table 1 for a list of SNPs, minor allele frequencies, and sample size information.

MR Image Acquisition

MRI acquisition was conducted using a quad split quadrature transmit/receive head coil on a GE Signa 3T scanner (Waukesha, WI). The resting state fMRI scan (8 minutes) was acquired during a multimodal imaging session that lasted 1 hour and 15 minutes. All participants were screened for MRI contraindications.

A T2*-weighted functional scan was acquired using an echo-planar pulse imaging (EPI) sequence (28 axial slices, 20 × 20 cm2 FOV, 64 × 64 matrix, 3.125 mm x 3.125 mm x 4 mm voxels, TE = 40 ms, TR = 2000 ms). The resting state fMRI scan was task-free, and individuals were told to close their eyes and "not think about anything in particular".

Resting State fMRI Processing and Analysis

Preprocessing was carried out in a similar fashion to what was previously published [35,36] using FSL [44] and AFNI [45], and in line with the methods used by the Human Connectome Project [46]. The first four volumes of the EPI data were removed followed by slice timing correction and despiking. Each volume was registered to the first volume and non-brain tissue was removed from the EPI data. To remove low-frequency drift from the

data a high pass filter (0.01 Hz) was applied, and the data were smoothed spatially using a 6-mm FWHM Gaussian filter.

To identify artefactual components in the data, independent components analysis (ICA) using FSL's MELODIC tool [47] was used on each participant's preprocessed data and the output for each participant included statistically independent spatial maps with associated time courses. This output was inspected for artefacts by two independent raters, and inter-rater agreement was high (Cohen's $\kappa = .85$). To denoise the data, these artefactual components were regressed out of each individual's data. The denoised data was then entered into a group ICA and 20 components were extracted. Of the 20 components, four components were visually identified as the aDMN, pDMN, FPN, and ECN (Supplementary Figure 1) and verified using a template-matching procedure [29, 36]. Dual regression [48, 49] was next performed to obtain individual time courses and spatial maps for statistical comparison.

Statistical Analysis

The association between genotype and functional connectivity was examined voxelwise using FSL's randomise tool [50] with 5000 permutations of nonparametric permutation testing. Each analysis was constrained to the voxels contained within the output ICA spatial map of the resting state network of interest. Consistent with past work [35, 36] separate ANOVAs were created for each SNP (Table 1). For SNPs with fewer than 10 minor allele homozygote carriers, dominant genetic models were used (i.e., two groups; minor allele carriers, including both homozygotes and heterozygotes, versus major allele homozygotes). An additive genetic model was used (i.e., three groups; minor allele homozygotes, heterozygotes, and major allele homozygotes) for SNPs with 10 or more minor allele homozygotes. For all models, age, sex, education, and *APOE*4 genotype were entered as covariates. SNP sequencing was not successful for all participants, leading to different sample sizes for each SNP of interest (Table 1). To account for missing data for each SNP test, one column per missing data point was added to the regression matrix and was considered as a variable of no interest (covariate) in the analysis. For any given SNP, this effectively removes the resting-state data and associated degrees of freedom from each participant with missing genotyping. Statistical maps output from FSL's randomise tool were cluster-corrected using threshold-free cluster enhancement [51]. Results are reported at family-wise error corrected $p < .05$ (voxel level) given *a priori* hypotheses, although strict Bonferroni correction would bring the p-value of $.05/30 = .002$ to account for the total number of SNPs tested, and a cluster size of ≥ 10 voxels [52].

RESULTS

Genotype Differences in Connectivity

A summary of the genotype-associated differences in connectivity can be found in Figure 1. Cluster-wise results for each statistically significant comparison are reported in Table 2 and voxel-wise comparison maps are presented in Supplementary Figure 2. All results are reported at $p < .05$ (cluster and family-wise error corrected) after controlling for age, sex, education, and *APOE4* genotype given the *a priori* hypotheses; with Bonferroni correction

for multiple comparisons, $p = .002$. Only the associations between *KIBRA* rs6555791 and pDMN connectivity survived stringent Bonferroni corrections ($p < .002$).

Additional models were run excluding *APOE4* genotype as a covariate (Supplementary Table 1). The results remain largely the same with a few exceptions. The associations between *KIBRA* rs6555802 and rs6555791 and connectivity were no longer observed (p's > .05). A relationship between *KIBRA* rs1030182 and aDMN connectivity was observed ($p < .05$), such that major allele homozygotes showed higher connectivity than minor allele homozygotes within the right superior frontal gyrus and right crus.

Anterior Default Mode Network—Major allele homozygotes of *BDNF* rs1491850 exhibited higher functional connectivity of the aDMN within the left frontal pole than heterozygotes ($p < .05$; additive model). Major allele homozygotes showed higher connectivity of the left putamen, posterior middle temporal gyrus, caudate, middle frontal gyrus, and anterior middle temporal gyrus than minor allele homozygotes within the aDMN ($p's < .05$; additive model). Heterozygotes of *KIBRA* rs6555791 exhibited higher functional connectivity of the aDMN compared to major allele homozygotes, with significant clusters dispersed across the network in frontal, parietal, and temporal lobes (see Table 2 for specific regions; additive model). There were no significant associations between aDMN connectivity and SNPs in *COMT*.

Posterior Default Mode Network—Major allele homozygotes of *BDNF* rs11030096 exhibited higher pDMN connectivity compared to heterozygotes in the left precuneus and cerebellum ($p's < .05$; additive model). *KIBRA* rs1030182 heterozygotes and major allele homozygotes exhibited higher connectivity than minor allele homozygotes in the right thalamus ($p's < .05$; additive model). Heterozygotes of *KIBRA* rs6555791 had higher connectivity than major allele homozygotes in the right posterior parahippocampal gyrus and inferior lateral occipital cortex and left superior lateral occipital cortex and posterior temporal fusiform cortex ($p's < .05$; additive model). Minor allele homozygotes of *KIBRA* rs6555791 had higher connectivity within the precuneus, left superior lateral occipital cortex and intracalcarine cortex than major allele homozygotes ($p's < .05$; additive model). Heterozygotes of *KIBRA* rs6555802 exhibited lower connectivity than major allele homozygotes within the right lingual gyrus of the pDMN ($p < .05$; additive model). There were no significant associations between connectivity within the pDMN and SNPs in *COMT*.

Executive Control Network—Minor allele carriers of *KIBRA* rs10475878 had lower functional connectivity than major allele homozygotes in the left frontal pole, caudate, and insular cortex of the ECN ($p's < .05$; dominant model). Heterozygotes of *KIBRA* rs6555791 exhibited higher connectivity in the left frontal cortex, frontal pole, and caudate ($p's < .05$; additive model) compared to major allele carriers. There were no significant associations between SNPs in *BDNF* or *COMT* and ECN connectivity.

Frontoparietal Network—Heterozygotes of *KIBRA* rs6555791 exhibited higher connectivity in the right middle frontal gyrus and left inferior frontal gyrus and bilaterally in the inferior temporal and superior lateral occipital gyrus ($p's < .05$; additive model)

compared to major allele homozygotes. There were no significant associations between SNPs in *BDNF* or *COMT* and connectivity within the FPN (p's > .05).

DISCUSSION

The purpose of the current study was to characterize the relationships between SNPs in *BDNF*, *COMT*, and *KIBRA* and functional connectivity of the DMN, ECN, and FPN in healthy, non-demented, middle-aged adults. We did not find an association between polymorphisms in *COMT* and functional connectivity in any of the networks investigated, but our results suggest relationships between connectivity within the FPN, ECN, aDMN, and pDMN and *BDNF* and *KIBRA* genes after controlling for age, sex, education, and *APOE4* genotype.

Our findings demonstrate a relationship between risk variants in *KIBRA* and *BDNF* and connectivity within the pDMN, aDMN, and ECN. The literature examining *KIBRA* has largely focused on the rs17070145 polymorphism, a common T to C substitution within the ninth intron of the gene. This SNP is associated with episodic memory performance [15] and moderately with AD [12]. *BDNF* has received attention as a candidate risk gene for AD due to its role in synaptic plasticity and regulation of long-term potentiation [8, 54]. This proposition is supported by the evidence showing that alterations in BDNF levels can affect brain integrity and ultimately cognition. For example, lower expression of BDNF proteins evident in mild cognitive impairment and AD patients is linked to worse cognitive function [55]. A common polymorphism within *BDNF* (Val66Met), which causes a significant decrease in activity-dependent release of BDNF, is associated with altered hippocampal integrity [16, 56, 57], DMN functional connectivity [58], and worse episodic memory [16, 56, 59]. Driscoll and colleagues [9] recently extended these findings by demonstrating a relationship between other *KIBRA* (rs6555802 and rs10475878) and *BDNF* (rs1491850) polymorphisms and probable dementia.

In the present study, risk allele carriers of *KIBRA* polymorphisms (rs6555802 [A allele]; rs10475878 [A allele]) previously associated with dementia risk [9] show hypoconnectivity within the posterior DMN (i.e., cluster encompassing precuneus) and ECN. Specifically, we observed that heterozygotes (AC) of *KIBRA* rs655802 had lower connectivity within the precuneus region of the pDMN than major allele homozygotes (CC; tested using additive model). Lower connectivity of the precuneus is largely in line with the existing literature reporting functional brain alterations in AD [17, 22, 24–26, 60]. The precuneus region serves as a cortical hub, working to integrate and rapidly disseminate functionally specific information [20]. This greatly connected hub region has high metabolic demands [61] and is vulnerable to early accumulation of Aß pathology [62, 63]. As a result, the precuneus is among one of the earliest regions to exhibit disrupted connectivity in AD [26]. We also report lower frontal connectivity of the ECN in minor risk allele carriers (AA/AG) of *KIBRA* rs10475878 compared to major allele homozygotes (GG; tested using dominant model). Though we expected to observe higher frontal connectivity in the ECN networks, based on the literature reporting altered patterns of connectivity in AD [24, 26, 31], our results are in accordance with reports of lower frontal connectivity observed in static resting state fMRI in the aging literature [64, 65]. In older adulthood, lower static

connectivity of the anterior regions is shown to be attributed to changes in the dynamics of anterior connections. More specifically, dynamic approaches, which take advantage of the time-varying aspect of functional connectivity rather than averaging across the full session, find that frontal regions display increased variability (i.e., flexibility) in their connectivity profiles across the scan period, which when analyzed using an average static approach, appeared as lower global static FC [65]. This shift in anterior brain dynamics (i.e., widespread frontal recruitment) is proposed to be a compensatory mechanism meant to accommodate for alterations in posterior connectivity (e.g., precuneus/PCC) and is in line with evidence from the task-based fMRI literature showing that frontal regions are more widely recruited in older compared to young adults to support successful cognitive performance [66, 67]. Taken together, our results suggest that variants in *KIBRA* may increase risk for AD through advancing neural age, such that frontal systems encompass a more compensatory signature of activity earlier in the aging trajectory (i.e., middle age) to overcome lower connectivity in critical posterior hubs (i.e., precuneus. Though more work is needed to discern the mechanisms underlying risk of pathological age-related cognitive decline conferred by SNPs in *KIBRA*, our results provide evidence that even after controlling for *APOE4*, the strongest genetic risk factor for AD, risk variants in *KIBRA* genes are associated with disrupted connectivity in functional networks related to episodic memory and executive function that can be observed in middle age.

In addition to disruptions in connectivity related to *KIBRA* and *BDNF variants*, we also report altered DMN, ECN, and FPN connectivity in less commonly studied polymorphisms of *BDNF* (rs11030096) and *KIBRA* (rs1030182, rs6555791). *BDNF* rs11030096 was associated with differences in DMN connectivity within the precuneus while *KIBRA* SNPs, in particular rs6555791, were associated with widespread alterations across all networks assessed. Although more work is necessary to characterize the role of *BDNF* rs11030096 and *KIBRA* rs1030182 and rs6555791 in aging and AD, our results suggest that functional connectivity measures are sensitive to genotype-related differences in major resting state networks underlying cognition and implicated in disease, in a healthy, non-demented middle-aged sample.

In the current study, we found no *COMT*-related differences in network connectivity in healthy middle-aged adults. *COMT* has been posited as a candidate gene for dementia considering its role in modulating prefrontal cognition, such as executive function, through degradation of dopamine [68]. The relationship between dopamine and cognition is proposed to exhibit an inverted U-shape, where dopamine activity above and below an optimal threshold negatively impacts prefrontal cognitive performance [69, 70]. Polymorphisms within *COMT,* including the Val to Met substitution at codon 158 on chromosome 22q11 (Val158Met), affect the level of dopamine activity. The Met allele has diminished catabolism of dopamine compared to Val resulting in prolonged dopamine exposure, benefitting prefrontal performance in Met carriers [71]. Young adulthood and middle age may mark a period in the lifespan where COMT polymorphisms exert minimal influence [71,72]. Our findings add to this growing literature and suggest that the influence of *COMT* polymorphisms on intermediate phenotypes of cognition are not evident in middle age (age 40–60), and that more sensitive techniques may be necessary to detect any subtle effects. Compared to young adulthood and middle age, the literature suggests

that the magnitude of the Val158Met effect on cognition is more pronounced in older adulthood [70] due to age-related changes to the dopamine system. More work is needed to determine the relationship between *COMT*, brain integrity, and cognition across the lifespan but particularly in older adulthood, when the dopamine system experiences age-related alterations and individuals are at greater risk for AD.

This study has several important limitations. Our study is limited by sample size. Overall, we had 123 participants with a comprehensive panel of genetic data (Table 1), though the number of complete observations for any given SNP was as low as 90. However, genetic-phenotype studies are typically conducted in larger samples (e.g., hundreds to thousands) to provide sufficient power [9]. It will be important to confirm the endophenotypes observed in the current investigation in larger, independent samples. The cross-sectional design is an additional limitation of the study. It will be critical for this line of research to follow individuals longitudinally to identify AD-converters and correspondingly, which genotype-related alterations in connectivity preclinically may represent pathological aging. Nevertheless, the limitations should not undermine the strengths of the current investigation including the use of a hypothesis-driven neuroimaging genetics approach in middle age to examine intermediate phenotypes of genetic polymorphisms that have been associated with AD. While some have criticized the candidate gene approach for potentially generating false positives because of the risk of an inflated type I error [73], hypothesis-driven candidate gene studies are important to validate GWAS findings and explore the intermediate biological phenotypes between behavior and disease.

In conclusion, we report significant associations between polymorphisms in *BDNF* and *KIBRA* with aDMN, pDMN, ECN, and FPN connectivity. This novel investigation documents the relationships between genetic polymorphisms in *BDNF* and *KIBRA* with connectivity in networks related to episodic memory and executive function in middle age. Further work using an endophenotype approach is necessary to better understand how genetic variants potentially contribute to AD risk and to identify preclinical biomarkers.

Supplementary Material

Refer to Web version on PubMed Central for supplementary material.

ACKNOWLDEGMENTS

This work was supported by the National Institute on Aging (NIA) R00-AG032361 (Driscoll).

REFERENCES

[1]. Alzheimer’s Association (2020) 2020 Alzheimer’s disease facts and figures. Alzheimers Dement 16, 391–460. 10.1002/alz.12068

[2]. Crous-Bou M, Minguillón C, Gramunt N, Molinuevo JL (2017) Alzheimer’s disease prevention: from risk factors to early intervention. Alzheimers Res Ther 9, 71. 10.1186/s13195-017-0297-z [PubMed: 28899416]

[3]. Hebert LE, Weuve J, Scherr PA, Evans A (2013) Alzheimer disease in the United States (2010–2050) estimated using the 2010 census. Neurology 80, 1778–1783. 10.1212/WNL.0b013e31828726f5 [PubMed: 23390181]

[4]. Deary IJ, Penke L, Johnson W (2010) The neuroscience of human intelligence differences. Nat Rev Neurosci 11, 201–211. 10.1038/nrn2793 [PubMed: 20145623]

[5]. McClearn GE, Johansson B, Berg S, Pedersen NL, Ahern F, Petrill SA, Plomin R (1997) Substantial genetic influence on cognitive abilities in twins 80 or more years old. Science 276, 1560–1563. 10.1126/science.276.5318.1560 [PubMed: 9171059]

[6]. Grober E, Hall CB, Lipton RB, Zonderman AB, Resnick SM, Kawas C (2008) Memory impairment, executive dysfunction, and intellectual decline in preclinical Alzheimer's disease. J Int Neuropsych Soc 14, 266–278. 10.1017/S1355617708080302

[7]. Hall CB, Ying J, Kuo L, Sliwinski M, Buschke H, Katz M, Lipton RB (2001) Estimation of bivariate measurements having different change points, with application to cognitive ageing. Stat Med 20, 3695–3714. 10.1002/sim.1113 [PubMed: 11782027]

[8]. Budni J, Bellettini-Santos T, Mina F, Garcez ML, Zugno AI (2015) The involvement of BDNF, NGF and GDNF in aging and Alzheimer's disease. Aging Dis 6, 331–341. 10.14336/AD.2015.0825 [PubMed: 26425388]

[9]. Driscoll I, Snively BM, Espeland MA, Shumaker SA, Rapp SR, Goveas JS, Casanova RL, Wactaawski-Wende J, Manson JE, Rossom R, Brooks J, Hernandez DG, Singleton AB, Resnick SM (2019) A candidate gene study of risk for dementia in older, postmenopausal women: Results from the Women's Health Initiative Memory Study. Int J Geriatr Psych 34, 692–699. 10.1002/gps.5068

[10]. Fukumoto N, Fujii T, Combarros O, Kamboh MI, Tsai SJ, Matsushita S, Nacmias B, Comings DE, Arboleda H, Ingelsson M, Hyman BT, Akatsu H, Grupe A, Nishimura AL, Zatz M, Mattila KM, Rinne J, Goto Y, Asada T, Nakamura S, Kunugi H (2010) Sexually dimorphic effect of the Val66Met polymorphism of BDNF on susceptibility to Alzheimer's disease: New data and meta-analysis. Am J Med Genet B 153, 235–242. 10.1002/ajmg.b.30986

[11]. Li GD, Bi R, Zhang DF, Xu M, Luo R, Wang D, Alzheimer's Disease Neuroimaging Initiative (ADNI), Fang Y, Li T, Zhang C, Yao Y (2017) Female-specific effect of the BDNF gene on Alzheimer's disease. Neurobiol Aging 53, 192.e11–192.e19. 10.1016/j.neurobiolaging.2016.12.023

[12]. Ling J, Huang Y, Zhang L, Wei D, Cheng W (2018) Association of KIBRA polymorphism with risk of Alzheimer's disease: evidence based on 20 case-control studies. Neurosci Lett 662, 77–83. 10.1016/j.neulet.2017.08.057 [PubMed: 28859866]

[13]. Serretti A, Olgiati P (2012) Catechol-o-methyltransferase and Alzheimer's disease: a review of biological and genetic findings. CNS Neurol Disord-Dr 11, 299–305. 10.2174/187152712800672472

[14]. Conner JM, Lauterborn JC, Yan Q, Gall CM, Varon S (1997) Distribution of brain-derived neurotrophic factor (BDNF) protein and mRNA in the normal adult rat CNS: evidence for anterograde axonal transport. J Neurosci 17, 2295–2313. 10.1523/JNEUROSCI.17-07-02295.1997 [PubMed: 9065491]

[15]. Papassotiropoulos A, Stephan DA, Huentelman MJ, Hoerndli FJ, Craig DW, Pearson JV, Huynh K, Brunner F, Corneveaux J, Osborne D, Wollmer MA, Aerni A, Coluccia D, Hänggi J, Mondadori CRA, Buchmann A, Reiman EM, Caselli RJ, Henke K, de Quervain DJF (2006) Common Kibra alleles are associated with human memory performance. Science 314, 475–478. 10.1126/science.1129837 [PubMed: 17053149]

[16]. Egan MF, Kojima M, Callicott JH, Goldberg TE, Kolachana BS, Bertolino A, Zaitsev E, Gold B, Goldman D, Dean M, Lu B, Weinberger DR (2003) The BDNF val66met polymorphism affects activity-dependent secretion of BDNF and human memory and hippocampal function. Cell 112, 257–269. 10.1016/S0092-8674(03)00035-7 [PubMed: 12553913]

[17]. Badhwar A, Tam A, Dansereau C, Orban P, Hoffstaedter F, Bellec P (2017) Resting-state network dysfunction in Alzheimer's disease: a systematic review and meta-analysis. Alzheimers Dement: DADM 8, 73–85. 10.1016/j.dadm.2017.03.007 [PubMed: 28560308]

[18]. Hohenfeld C, Werner CJ, Reetz K (2018) Resting-state connectivity in neurodegenerative disorders: Is there potential for an imaging biomarker?. NeuroImage-Clin 18, 849–870. 10.1016/j.nicl.2018.03.013 [PubMed: 29876270]

[19]. Wisch JK, Roe CM, Babulal GM, Schindler SE, Fagan AM, Benzinger TL, Morris JC, Ances BM (2020) Resting state functional connectivity signature differentiates cognitively normal from

individuals who convert to symptomatic alzheimer's disease. J Alzheimers Dis 74, 1085–1095. 10.3233/JAD-191039 [PubMed: 32144983]

[20]. Buckner RL, Sepulcre J, Talukdar T, Krienen FM, Liu H, Hedden T, Andrews-Hanna JR, Sperling RA, Johnson, KA (2009) Cortical hubs revealed by intrinsic functional connectivity: mapping, assessment of stability, and relation to Alzheimer's disease. J Neurosci 29, 1860–1873. 10.1523/JNEUROSCI.5062-08.2009 [PubMed: 19211893]

[21]. Andrews-Hanna JR, Reidler JS, Sepulcre J, Poulin R, Buckner RL (2010). Functional-anatomic fractionation of the brain's default network. Neuron 65, 550–562. 10.1016/j.neuron.2010.02.005 [PubMed: 20188659]

[22]. Damoiseaux JS, Prater KE, Miller BL, Greicius MD (2012) Functional connectivity tracks clinical deterioration in Alzheimer's disease. Neurobiol Aging 33, 828.e19–828.e30. 10.1016/j.neurobiolaging.2011.06.024

[23]. Yuan B, Xie C, Shu H, Liao W, Wang Z, Liu D, Zhang Z (2016) Differential effects of APOE genotypes on the anterior and posterior subnetworks of default mode network in amnestic mild cognitive impairment. J Alzheimers Dis 54, 1409–1423. 10.3233/JAD-160353 [PubMed: 27589521]

[24]. Agosta F, Pievani M, Geroldi C, Copetti M, Frisoni GB, Filippi M (2012) Resting state fMRI in Alzheimer's disease: beyond the default mode network. Neurobiol Aging 33, 1564–1578. 10.1016/j.neurobiolaging.2011.06.007 [PubMed: 21813210]

[25]. Gour N, Felician O, Didic M, Koric L, Gueriot C, Chanoine V, Confort-Gouny S, Guye M, Ceccaldi M, Ranjeva JP (2014) Functional connectivity changes differ in early and late-onset alzheimer's disease. Hum Brain Mapp 35, 2978–2994. 10.1002/hbm.22379 [PubMed: 24123475]

[26]. Jones DT, Knopman DS, Gunter JL, Graff-Radford J, Vemuri P, Boeve BF, Petersen RC, Weiner MW, Jack CR Jr (2016) Cascading network failure across the Alzheimer's disease spectrum. Brain 139, 547–562. 10.1093/brain/awv338 [PubMed: 26586695]

[27]. Palmqvist S, Schöll M, Strandberg O, Mattsson N, Stomrud E, Zetterberg H, Blennow K, Landau S, Jagust W, Hansson O (2017) Earliest accumulation of β-amyloid occurs within the default-mode network and concurrently affects brain connectivity. Nat Commun 8, 1214. 10.1038/s41467-017-01150-x [PubMed: 29089479]

[28]. Matura S, Prvulovic D, Butz M, Hartmann D, Sepanski B, Linnemann K, Oertel-Knöchel V, Karakaya T, Fußer F, Pantel J, van de Ven V (2014) Recognition memory is associated with altered resting-state functional connectivity in people at genetic risk for Alzheimer's disease. Eur J Neurosci 40, 3128–3135. 10.1111/ejn.12659 [PubMed: 24989884]

[29]. Smith SM, Fox PT, Miller KL, Glahn DC, Fox PM, Mackay CE, Filippini N, Watkins KE, Toro R, Laird AR, Beckmann CF (2009) Correspondence of the brain's functional architecture during activation and rest. P Natl Acad Sci USA 106, 13040–13045. 10.1073/pnas.0905267106

[30]. Zhang HY, Wang SJ, Liu B, Ma ZL, Yang M, Zhang ZJ, Teng GJ (2010) Resting brain connectivity: changes during the progress of Alzheimer disease. Radiology 256, 598–606. 10.1148/radiol.10091701 [PubMed: 20656843]

[31]. Zhao Q, Lu H, Metmer H, Li WX, Lu J (2018) Evaluating functional connectivity of executive control network and frontoparietal network in Alzheimer's disease. Brain Res 1678, 262–272. 10.1016/j.brainres.2017.10.025 [PubMed: 29079506]

[32]. Goveas JS, Xie C, Chen G, Li W, Ward BD, Franczak MB, Jones JL, Antuono PG, Li SJ (2013) Functional network endophenotypes unravel the effects of apolipoprotein E epsilon 4 in middle-aged adults. PloS One 8, e55902–e55902. 10.1371/journal.pone.0055902 [PubMed: 23424640]

[33]. Patel KT, Stevens MC, Pearlson GD, Winkler AM, Hawkins KA, Skudlarski P, Bauer LO (2013) Default mode network activity and white matter integrity in healthy middle-aged ApoE4 carriers. Brain Imaging Behav 7, 60–67. 10.1007/s11682-012-9187-y [PubMed: 23011382]

[34]. Dowell NG, Evans SL, Tofts PS, King SL, Tabet N, Rusted JM (2016) Structural and resting-state MRI detects regional brain differences in young and mid-age healthy APOE-e4 carriers compared with non-APOE-e4 carriers. NMR Biomed 29, 614–624. 10.1002/nbm.3502 [PubMed: 26929040]

[35]. Korthauer LE, Zhan L, Ajilore O, Leow A, Driscoll I (2018) Disrupted topology of the resting state structural connectome in middle-aged APOE ε4 carriers. Neuroimage 178, 295–305. 10.1016/j.neuroimage.2018.05.052 [PubMed: 29803958]

[36]. Blujus JK, Korthauer LE, Awe E, Frahmand M, Driscoll I (2020) Single Nucleotide Polymorphisms in Alzheimer's Disease Risk Genes Are Associated with Intrinsic Connectivity in Middle Age. J Alzheimers Dis 78, 309–320. 10.3233/JAD-200444 [PubMed: 32986668]

[37]. Franzmeier N, Ren J, Damm A, Monté-Rubio G, Boada M, Ruiz A, Ramirez A, Jessen F, Düzel E, Gómez OR, Benzinger T, Goate A, Karch CM, Fagan AM, McDade E, Buerfer K, Levin J, Duering M, Dichgans M, Suárez-Calvet M, Haass C, Gordon BA, Lim YY, Masters CL, Janowitz D, Catak C, Wolfsgruber S, Wagner M, Milz E, Moreno-Grau S, Teipel S, Grothe MJ, Kilimann I, Rossor M, Fox N, Laske C, Chhatwal J, Falkai P, Perneczky R, Lee J, Spottke A, Boecker H, Brosseron F, Fliessbach K, Heneka MT, Nestor P, Peters O, Fuentes M, Menne F, Priller J, Spruth EJ, Franke C, Schneider A, Westereicher C, Speck O, Wiltfang J, Bartels C, Caballero MÁA, Metzger C, Bittner D, Salloway S, Danek A, Hassenstab J, Yakushev I, Schofield PR, Morris JC, Bateman RJ, Ewers M (2019) The BDNF Val66Met SNP modulates the association between beta-amyloid and hippocampal disconnection in Alzheimer's disease. Mol Psychiatr 26, 614–628. 10.1038/s41380-019-0404-6

[38]. Liu B, Song M, Li J, Liu Y, Li K, Yu C, Jiang T (2010) Prefrontal-related functional connectivities within the default network are modulated by COMT val158met in healthy young adults. J Neurosci 30, 64–69. 10.1523/JNEUROSCI.3941-09.2010 [PubMed: 20053888]

[39]. Tunbridge EM, Farrell SM, Harrison PJ, Mackay CE (2013) Catechol-O-methyltransferase (COMT) influences the connectivity of the prefrontal cortex at rest. Neuroimage 68, 49–54. 10.1016/j.neuroimage.2012.11.059 [PubMed: 23228511]

[40]. Zhang N, Liu H, Qin W, Liu B, Jiang T, Yu C (2017) APOE and KIBRA interactions on brain functional connectivity in healthy young adults. Cereb Cortex 27, 4797–4805. 10.1093/cercor/bhw276 [PubMed: 27620974]

[41]. Jurica PJ, Leitten CL, Mattis S (2004) DRS-2 Dementia Rating Scale-2: Professional Manual. Psychological Assessment Resources.

[42]. Folstein MF, Folstein SE, McHugh PR (1975) "Mini-mental state": a practical method for grading the cognitive state of patients for the clinician. J Psychiat Res 12, 189–198. [PubMed: 1202204]

[43]. Yesavage JA, Brink TL, Rose TL, Lum O, Huang V, Adey M, Leirer VO (1982) Development and validation of a geriatric depression screening scale: a preliminary report. J Psychiat Res 17, 37–49. [PubMed: 7183759]

[44]. Smith SM, Jenkinson M, Woolrich MW, Beckmann CF, Behrens TE, Johansen-Berg H, Bannister PR, De Luca M, Drobnjak I, Flitney DE, Niazy RK, Saunders J, Vickers J, Zhang Y, De Stefano N, Brady JM, Matthews PM (2004) Advances in functional and structural MR image analysis and implementation as FSL. Neuroimage 23, S208–S219. 10.1016/j.neuroimage.2004.07.051 [PubMed: 15501092]

[45]. Cox RW (1996) AFNI: software for analysis and visualization of functional magnetic resonance neuroimages. Comput Biomed Res 29, 162–173. 10.1006/cbmr.1996.0014 [PubMed: 8812068]

[46]. Smith SM, Beckmann CF, Andersson J, Auerbach EJ, Bijsterbosch J, Douaud G, Duff E, Feinberg DA, Griffanti L, Harms MP, Kelly M, Laumann T, Miller KL, Moeller S, Petersen S, Power J, Salimi-Khorshidi G, Snyder AZ, Vu AT, Woorich MW, Xu J, Yacoub E, Uğurbilb K, Van Essen DC, Glasser MF (2013) Resting-state fMRI in the human connectome project. Neuroimage 80, 144–168. 10.1016/j.neuroimage.2013.05.039 [PubMed: 23702415]

[47]. Beckmann CF, DeLuca M, Devlin JT, Smith SM (2005) Investigations into resting-state connectivity using independent component analysis. Philos T R Soc B 360, 1001–1013. 10.1098/rstb.2005.1634

[48]. Beckmann CF, Mackay CE, Filippini N, Smith SM (2009) Group comparison of resting-state FMRI data using multi-subject ICA and dual regression. Neuroimage 47, S148. 10.1016/S1053-8119(09)71511-3

[49]. Nickerson LD, Smith SM, Öngür D, Beckmann CF (2017) Using dual regression to investigate network shape and amplitude in functional connectivity analyses. Front Neurosci-Switz 11, 115. 10.3389/fnins.2017.00115

[50]. Winkler AM, Ridgway GR, Webster MA, Smith SM, Nichols TE (2014) Permutation inference for the general linear model. Neuroimage 92, 381–397. 10.1016/j.neuroimage.2014.01.060 [PubMed: 24530839]

[51]. Smith SM, Nichols TE (2009) Threshold-free cluster enhancement: addressing problems of smoothing, threshold dependence and localisation in cluster inference. Neuroimage 44, 83–98. 10.1016/j.neuroimage.2008.03.061 [PubMed: 18501637]

[52]. Damoiseaux JS, Seeley WW, Zhou J, Shirer WR, Coppola G, Karydas A, Rosen HJ, Miller BL, Kramer JH,, Greicius MD (2012) Gender modulates the APOE ε4 effect in healthy older adults: convergent evidence from functional brain connectivity and spinal fluid tau levels. J Neurosci 32, 8254–8262. 10.1523/JNEUROSCI.0305-12.2012 [PubMed: 22699906]

[53]. Faul F, Erdfelder E, Lang AG, Buchner A (2007) G* Power 3: A flexible statistical power analysis program for the social, behavioral, and biomedical sciences. Behav Res Methods 39, 175–191. 10.3758/BF03193146 [PubMed: 17695343]

[54]. Lu B, Nagappan G, Guan X, Nathan PJ, Wren P (2013) BDNF-based synaptic repair as a disease-modifying strategy for neurodegenerative diseases. Nat Rev Neurosci 14, 401–416. 10.1038/nrn3505 [PubMed: 23674053]

[55]. Peng S, Wuu J, Mufson EJ, Fahnestock M (2005) Precursor form of brain-derived neurotrophic factor and mature brain-derived neurotrophic factor are decreased in the pre-clinical stages of Alzheimer's disease. J Neurochem 93, 1412–1421. 10.1111/j.1471-4159.2005.03135.x [PubMed: 15935057]

[56]. Kambeitz JP, Bhattacharyya S, Kambeitz-Ilankovic LM, Valli I, Collier DA, McGuire P (2012) Effect of BDNF val66met polymorphism on declarative memory and its neural substrate: A meta-analysis. Neurosci Biobehav R 36, 2165–2177. 10.1016/j.neubiorev.2012.07.002

[57]. Lim YY, Rainey-Smith S, Lim Y, Laws SM, Gupta V, Porter T, Bourgeat P, Ames D, Fowler C, Salvado O, Villemagne VL, Rowe CC, Masters CL, Zhou XF, Martins RN, Maruff P (2017) BDNF Val66Met in preclinical Alzheimer's disease is associated with short-term changes in episodic memory and hippocampal volume but not serum mBDNF. Int Psychogeriatr 29, 1825–1834. 10.1017/S1041610217001284 [PubMed: 28720165]

[58]. Lin PH, Tsai SJ, Huang CW, Mu-En L, Hsu SW, Lee CC, Chen NC, Chang YT, Luan MY, Chang CC (2016) Dose-dependent genotype effects of BDNF Val66Met polymorphism on default mode network in early stage Alzheimer's disease. Oncotarget 7, 54200–54214. 10.18632/oncotarget.11027 [PubMed: 27494844]

[59]. Azeredo LAD, De Nardi T, Levandowski ML, Tractenberg SG, Kommers-Molina J, Wieck A, Irigaray TQ, da Silva Filho IG, Grassi-Oliveira R (2017) The brain-derived neurotrophic factor (BDNF) gene Val66Met polymorphism affects memory performance in older adults. B J Psychiatr 39, 90–94. 10.1590/1516-4446-2016-1980

[60]. Balthazar ML, Pereira FR, Lopes TM, da Silva EL, Coan AC, Campos BM, Duncan NW, Stella F, Northoff G, Damasceno BP, Cendes F (2014) Neuropsychiatric symptoms in Alzheimer's disease are related to functional connectivity alterations in the salience network. Hum Brain Mapp 35, 1237–1246. 10.1002/hbm.22248 [PubMed: 23418130]

[61]. Tomasi D, Wang GJ, Volkow ND (2013) Energetic cost of brain functional connectivity. P Natl A Sci USA 110, 13642–13647. 10.1073/pnas.1303346110

[62]. Oh H, Madison C, Baker S, Rabinovici G, Jagust W (2016) Dynamic relationships between age, amyloid-β deposition, and glucose metabolism link to the regional vulnerability to Alzheimer's disease. Brain 139, 2275–2289. 10.1093/brain/aww108 [PubMed: 27190008]

[63]. Palmqvist S, Schöll M, Strandberg O, Mattsson N, Stomrud E, Zetterberg H, Blennow K, Landau S, Jagust W, Hansson O (2017) Earliest accumulation of β-amyloid occurs within the default-mode network and concurrently affects brain connectivity. Nat Commun 8, 1–13. 10.1038/s41467-017-01150-x [PubMed: 28232747]

[64]. Onoda K, Ishihara M, Yamaguchi S (2012) Decreased Functional Connectivity by Aging Is Associated with Cognitive Decline. J Cognitive Neurosci 24, 2186–2198. 10.1162/jocn_a_00269

[65]. Zhang H, Lee A, Qiu A (2017) A posterior-to-anterior shift of brain functional dynamics in aging. Brain Struct Funct 222, 3665–3676. 10.1007/s00429-017-1425-z [PubMed: 28417233]

[66]. Grady CL, McIntosh AR, Craik FI (2005) Task-related activity in prefrontal cortex and its relation to recognition memory performance in young and old adults. Neuropsychologia 43, 1466–1481. 10.1016/j.neuropsychologia.2004.12.016 [PubMed: 15989937]

[67]. Reuter-Lorenz PA, Jonides J, Smith EE, Hartley A, Miller A, Marshuetz C, Koeppe RA (2000) Age Differences in the Frontal Lateralization of Verbal and Spatial Working Memory Revealed by PET. Journal of Cognitive Neuroscience 12, 174–187. 10.1162/089892900561814 [PubMed: 10769314]

[68]. Dickinson D, Elvevåg B. (2009). Genes, cognition and brain through a COMT lens. Neuroscience 164, 72–87. 10.1016/j.neuroscience.2009.05.014 [PubMed: 19446012]

[69]. Mattay VS, Goldberg TE, Fera F, Hariri AR, Tessitore A, Egan MF, Kolachana B, Callicott JH, Weinberger DR (2003) Catechol O-methyltransferase val158-met genotype and individual variation in the brain response to amphetamine. P Natl Acad Sci USA 100, 6186–6191. 10.1073/pnas.0931309100

[70]. Nagel IE, Chicherio C, Li SC, Von Oertzen T, Sander T, Villringer A, Heekeren HR, Bäckman L, Lindenberger U (2008) Human aging magnifies genetic effects on executive functioning and working memory. Front Hum Neurosci 2, 1. 10.3389/neuro.09.001.2008 [PubMed: 18958202]

[71]. Egan MF, Goldberg TE, Kolachana BS, Callicott JH, Mazzanti CM, Straub RE, Goldman D, Weinberger DR (2001) Effect of COMT Val108/158 Met genotype on frontal lobe function and risk for schizophrenia. P Natl Acad Sci USA 98, 6917–6922. 10.1073/pnas.111134598

[72]. Frias CMD, Annerbrink K, Westberg L, Eriksson E, Adolfsson R, Nilsson LG (2005) Catechol O-methyltransferase Val158Met polymorphism is associated with cognitive performance in nondemented adults. J Cognitive Neurosci 17, 1018–1025. 10.1162/0898929054475136

[73]. Jorgensen TJ, Ruczinski I, Kessing B, Smith MW, Shugart YY, Alberg AJ (2009) Hypothesis-driven candidate gene association studies: practical design and analytical considerations. Am J Epidemiol 170, 986–993. 10.1093/aje/kwp242 [PubMed: 19762372]

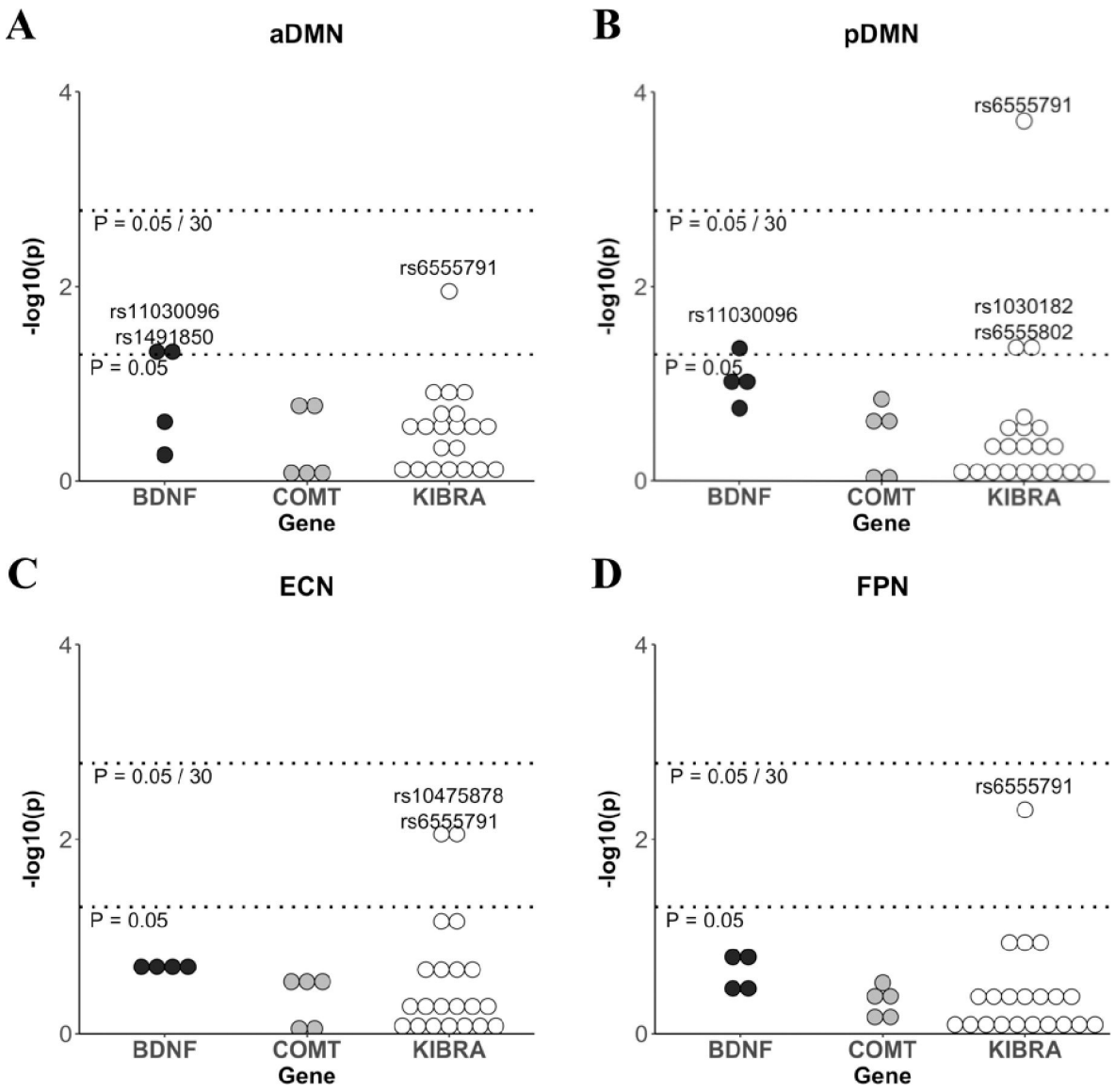

Figure 1.

Plot displays statistical associations between SNPs and functional connectivity within each resting state network of interest. Each dot represents a polymorphism in BDNF, COMT, or KIBRA (see Table 1 for listing). Dots above the p-value line of .05 represents SNPs that showed statistically significant associations with connectivity in the (A) aDMN; (B) pDMN; (C) ECN; and (D) FPN. Dots above the p-value line of .05/30 represent statistical associations that survived Bonferroni correction. All models controlled for age, sex, education, and APOE genotype. Connectivity within the aDMN, pDMN, ECN, and FPN are related to polymorphisms within BDNF (rs11030096, rs1491850) and KIBRA (rs1030182, rs10475878, rs6555791, rs6555802). Findings related to BDNF rs11030096 and aDMN connectivity were not reported in the results section as the cluster size was less than 10 voxels.

Abbreviations: aDMN = anterior default mode network; pDMN = posterior default mode network; ECN = executive control network; FPN = frontoparietal network.

Table 1.

Sample SNP Information.

Gene/SNP	Alleles	Minor Allele	Minor Homozygotes N (%)	Heterozygotes N (%)	Major Homozygotes N (%)	*APOE4* Carriers N (%)	Complete Observations	Analysis Model
BDNF								
rs11030096	CT	C	26 (22.03%)	59 (50.00%)	33 (27.97%)	34 (28.81%)	115	Additive
rs1491850	CT	C	20 (16.26%)	65 (52.85%)	38 (30.89%)	34 (27.64%)	120	Additive
rs6265	AG	A	6 (6.52%)	23 (25.00%)	63 (68.48%)	26 (28.26%)	90	Dominant
rs985205	AT	A	1 (0.94%)	35 (33.02%)	70 (66.04%)	27 (25.47%)	103	Dominant
COMT								
rs1544325	AG	A	13 (11.30%)	66 (57.39%)	36 (31.30%)	34 (29.57%)	113	Additive
rs4633	CT	T	34 (28.33%)	48 (40.00%)	38 (31.67%)	34 (28.33%)	117	Additive
rs4646316	CT	T	5 (4.20%)	57 (47.90%)	57 (47.90%)	33 (27.73%)	116	Dominant
rs4680 *	AG	A	29 (29.00%)	41 (41.00%)	30 (30.00%)	24 (24.00%)	98	Additive
rs737865	CT	C	11 (9.09%)	57 (47.11%)	53 (43.80%)	34 (28.10%)	119	Additive
KIBRA								
rs10040267	AG	A	26 (22.03%)	50 (42.37%)	42 (35.59%)	34 (28.81%)	115	Additive
rs1030182	AG	A	24 (19.67%)	57 (46.72%)	41 (33.61%)	34 (27.87%)	119	Additive
rs10475878	AG	A	7 (5.88%)	50 (42.02%)	62 (52.10%)	34 (28.57%)	116	Dominant
rs11134509	AG	A	15 (12.30%)	61 (50.00%)	46 (37.70%)	34 (27.87%)	119	Additive
rs11740112 *	AG	G	21 (19.27%)	53 (48.62%)	35 (32.11%)	31 (28.44%)	107	Additive
rs11750709	AG	A	12 (9.76%)	61 (49.59%)	50 (40.65%)	34 (27.64%)	120	Additive
rs13171394	AG	A	30 (25.00%)	55 (45.83%)	35 (29.17%)	33 (27.50%)	117	Additive
rs1422422 *	AG	A	10 (8.85%)	57 (50.44%)	46 (40.71%)	32 (28.32%)	110	Additive
rs1477306	AG	A	13 (10.92%)	52 (43.70%)	54 (45.38%)	33 (27.73%)	116	Additive
rs17070145	CT	T	13 (11.02%)	55 (46.61%)	50 (42.37%)	33 (27.97%)	115	Additive
rs2241368	CT	C	25 (20.66%)	27 (22.31%)	69 (57.02%)	34 (28.10%)	118	Additive
rs244904	AG	A	27 (22.31%)	64 (52.89%)	30 (24.79%)	34 (28.10%)	118	Additive
rs3822659	AC	C	0 (0.00%)	37 (30.08%)	86 (69.92%)	34 (27.64%)	120	Dominant
rs3822660	AC	A	0 (0.00%)	23 (20.00%)	92 (80.00%)	29 (25.22%)	112	Dominant

Gene/SNP	Alleles	Minor Allele	Minor Homozygotes N (%)	Heterozygotes N (%)	Major Homozygotes N (%)	*APOE4* Carriers N (%)	Complete Observations	Analysis Model
rs4320284	GT	G	15 (12.61%)	62 (52.10%)	42 (35.29%)	34 (28.57%)	116	Additive
rs4976592	CT	T	8 (6.72%)	53 (44.54%)	58 (48.74%)	33 (27.73%)	117	Dominant
rs6555791	AT	T	13 (10.66%)	62 (50.82%)	47 (38.52%)	34 (27.87%)	119	Additive
rs6555802	AC	A	12 (9.76%)	57 (46.34%)	54 (43.90%)	34 (27.64%)	120	Additive
rs764221	AG	A	13 (11.02%)	77 (65.25%)	28 (23.73%)	34 (28.81%)	115	Additive
rs7700355	CT	T	0 (0.00%)	31 (26.96%)	84 (73.04%)	32 (27.83%)	112	Dominant
rs7723533	AG	A	7 (5.69%)	40 (32.52%)	76 (61.79%)	34 (27.64%)	120	Dominant

Note. Dominant models consisted of two groups including minor allele carriers (i.e., minor allele homozygotes and heterozygotes) and major allele homozygotes and were employed when the sample size of minor allele homozygotes was less than 10. Additive models consisted of three groups (i.e., minor allele homozygotes, heterozygotes, major allele homozygotes) and were conducted when minor allele homozygote group size was greater than 10. *APOE4* carrier status is defined as individuals carrying 1 or 2 ε4 alleles. Complete observations indicate the number of complete datapoints (i.e., participants with full profile of genotype and covariate [age, sex, education, *APOE4*] data) entered to the regression for each SNP.

*Indicates SNPs that had less than 80% power to detect moderate-sized effects.

Table 2.

Summary of resting state fMRI functional connectivity findings by network and SNP.

						Peak Voxel MNI Coordinates (mm)			
Network	**Gene**	**SNP**	**Contrast**	**Brain Region**	**Brodmann Area (BA)**	***k***	**X**	**Y**	**Z**
aDMN	*BDNF*	rs1491850	Maj > Het	L Frontal Pole	BA9	183	−12	50	40
			Maj > Min	L Putamen	--	162	−22	2	8
			Maj > Min	L Posterior Middle Temporal Gyrus	BA21	41	−62	−42	−4
			Maj > Min	L Caudate	--	23	−8	10	14
			Maj > Min	L Middle Frontal Gyrus	BA9	19	−32	18	48
			Maj > Min	L Middle Frontal Gyrus	BA9	13	−42	10	48
			Maj > Min	L Anterior Middle Temporal Gyrus	BA21	12	−52	2	−28
	KIBRA	rs6555791	Het > Maj	L Paracingulate Gyrus	BA10	3877	−10	50	2
			Het > Maj	L Frontal Orbital Cortex	BA45	1121	−44	18	−10
			Het > Maj	L Anterior Middle Temporal Gyrus	BA20	1076	−52	−4	−32
			Het > Maj	L Middle Frontal Gyrus	BA44	252	−38	14	38
			Het > Maj	R Crus II	--	210	20	−78	−36
			Het > Maj	R Superior Frontal Gyrus	BA32	82	14	18	50
			Het > Maj	R Superior Parietal Lobule	BA40	77	36	−38	48
			Het > Maj	L Superior Lateral Occipital Cortex	BA39	72	−42	−62	24
			Het > Maj	R Superior Frontal Gyrus	BA6	41	14	4	58
			Het > Maj	L Frontal Pole	BA11	33	−28	58	2
			Het > Maj	L Posterior Middle Temporal Gyrus	BA21	30	−56	−42	−6

						Peak Voxel MNI Coordinates (mm)			
Network	**Gene**	**SNP**	**Contrast**	**Brain Region**	**Brodmann Area (BA)**	***k***	**X**	**Y**	**Z**
			Het > Maj	R Caudate	--	23	20	−8	20
			Het > Maj	R Postcentral Gyrus	BA3	21	34	−22	40
			Het > Maj	L Posterior Cingulate Gyrus	BA23	14	−6	−54	30
			Het > Maj	L Thalamus	--	12	−6	−4	4
pDMN	*BDNF*	rs11030096	Maj > Het	L Cerebellar V	--	148	0	−64	−6
			Maj > Het	L Precuneus	--	47	−8	−60	34
	KIBRA	rs1030182	Het > Min	R Thalamus	--	25	8	−16	6
			Maj > Min	R Thalamus	--	17	8	−14	4
	KIBRA	rs6555791	Het > Maj	R Posterior Parahippocampal Gyrus	BA27	8214	14	−38	−4
			Het > Maj	R Inferior Lateral Occipital Cortex	BA37	1350	52	−66	12
			Het > Maj	L Superior Lateral Occipital Cortex	BA39	907	−42	−76	22
			Het > Maj	L Posterior Temporal Fusiform Cortex	BA37	372	−26	−36	−20
			Min > Maj	R Precuneus Cortex	BA7	1394	2	−74	38
			Min > Maj	L Superior Lateral Occipital Cortex	BA39	36	−44	−66	32
			Min > Maj	L Intracalcarine Cortex	BA17	32	−22	−62	10
			Min > Maj	L Precuneus Cortex	BA23	17	−14	−58	24
	KIBRA	rs6555802	Maj > Het	R Lingual Gyrus	BA23	445	16	−58	2
ECN	*KIBRA*	rs10475878	Maj > Het	L Insular Cortex	BA47	145	−32	20	−4
			Maj > Het	L Frontal Pole	BA47	113	−26	40	−4
			Maj > Het	L Frontal Pole	BA11	32	−12	60	−6

						Peak Voxel MNI Coordinates (mm)			
Network	**Gene**	**SNP**	**Contrast**	**Brain Region**	**Brodmann Area (BA)**	***k***	**X**	**Y**	**Z**
			Maj > Het	L Caudate	--	25	−14	16	6
	KIBRA	rs6555791	Het > Maj	L Frontal Cortex	BA32	5797	−16	36	6
			Het > Maj	L Caudate	--	102	−18	14	12
			Het > Maj	L Frontal Pole	BA32	63	−16	38	30
FPN	*KIBRA*	rs6555791	Het > Maj	L Inferior Frontal Gyrus	BA48	3365	−42	16	16
			Het > Maj	L Superior Lateral Occipital Cortex	BA19	1837	−34	−84	28
			Het > Maj	L Inferior Temporal Gyrus	BA37	933	−50	−62	−22
			Het > Maj	R Superior Lateral Occipital Cortex	BA7	531	36	−66	42
			Het > Maj	R Inferior Temporal Gyrus	BA20	117	62	−48	−18
			Het > Maj	R Middle Frontal Gyrus	BA48	60	48	24	30

Threshold-free cluster enhancement and family-wise error corrected clusters significant at $p < .05$.

Abbreviations: *k* = cluster size; aDMN = anterior default mode network; pDMN = posterior default mode network; ECN = executive control network; min = minor allele homozygote; het = heterozygotes; maj = major allele homozygotes; BA = Brodmann Area.